tional parameters and their errors (Tables S2 and S7), thermal parameters (Tables S3 and S8), bond distances (Tables S4 and S9), bond angles (Tables S5 and S10), and electronic absorption spectral data (Table S11), and figures showing the full atomic number schemes for the monocations of **1** (Figure S1) and **2** (Figure S2) and the X-band ESR spectrum of $[Re_2Cl_3(\mu\text{-}HN_2C_2Me_2)(\mu\text{-dppm})_2(NCMe)]PF_6$ (Figure S3) (44 pages); tables of observed and calculated structure factors (82 pages). Ordering information is given on any current masthead page.

Contribution from the Departments of Chemistry, The University of Michigan,
Ann Arbor, Michigan 48109, and The University of Iowa, Iowa City, Iowa 52240

Protonation of the 1,1-Dithiolene Ligands in the $[Cu_8(L)_6]^{4-}$ Cubanes (L = $[S_2C{=}C(COOR)_2]^{2-}$) and Synthesis of the $[Cu_8(L)_{6-n}(H\text{-}L)_n]^{-(4-n)}$ Clusters. Synthesis and Structural Characterization of the $[Cu_{10}(H\text{-}L)_6(L)_2]$ Decanuclear Cluster

D. Coucouvanis,* D. Swenson, N. C. Baenziger, R. Pedelty, M. L. Caffery, and S. Kanodia

Received January 27, 1989

Addition of 1, 2, or 3 equiv of acid to CH_3CN solutions of the $K_4Cu_8(R_2DED)_6$ cubane cluster complexes ($R_2DED = [S_2C{=}C(COOR)_2]^{2-}$; R = Et (I), *t*-Bu (II)) by using standarized $HClO_4/CH_3CN$ solutions results in the formation of the protonated complexes $[Cu_8(L)_{6-n}(H\text{-}L)_n]^{-(4-n)}$ (L = Et_2DED, $n = 1, 2, 3$; L = *t*-Bu_2DED, $n = 1, 2$) that were isolated as crystalline tetraarylphosphonium or tetraalkylammonium salts. The protonated clusters can be titrated with standard base to give back the "parent" cubanes in quantitative yields. The cubane structure of the $[Cu_8(L)_5(H\text{-}L)]^{3-}$ (L = *t*-Bu_2DED) cluster has been established unequivocally by ^{13}C NMR spectroscopy. Upon addition of 4 equiv of acid to $K_4Cu_8(t\text{-}Bu_2DED)_6$, a red Cu(I) cluster of stoichiometry $[Cu_{10}(H\text{-}L)_6(L)_2]$ (L = *t*-Bu_2DED) forms and can be isolated in crystalline form (III). Neutral complex III crystallizes in the triclinic space group $P\bar{1}$ with one molecule per unit cell. The cell dimensions are $a = 14.435$ (3) Å, $b = 16.979$ (3) Å, $c = 14.843$ (3) Å, $\alpha = 98.16$ (4)°, $\beta = 108.90$ (2)°, $\gamma = 85.42$ (4)°. Intensity data were collected with a four-circle computer-controlled diffractometer using the θ–2θ scan technique. Refinement by full-matrix least-squares techniques of 374 parameters on 4284 data gave a final R value of 0.067. The copper framework in III consists of two Cu_4 subunits. Of the four ligands surrounding each of the Cu_4 subunits, three are protonated at the ethylenic carbon adjacent to the CS_2 unit ("methine" carbon) and can be considered dithio acid monoanions $(H\text{-}t\text{-}Bu_2DED)^-$. The fourth ligand is a 1,1-ethylenedithiolate dianion, $(t\text{-}Bu_2DED)^{2-}$. The latter connects the Cu_4 fragment to the bridging copper atom by coordination via oxygen and sulfur atoms. A third coordination site on the bridging copper is occupied by a dithio acid sulfur on the adjacent Cu_4 fragment. The coordination geometry about each of the copper atoms in the structure is distorted trigonal and nearly planar. Ranges of selected structural parameters are as follows: Cu–S, 2.230 (3)–2.322 (3) Å; Cu–Cu, 2.656 (2)–3.056 (2) Å; Cu–O, 1.898 (8) Å; S–Cu–S, 106.0 (1)–131.8 (1)°; Cu–S–C, 98.5 (4)–110.0 (4)°.

Introduction

The polynuclear aggregates obtained in reactions of Cu(I) with sulfur-containing ligands display a wide variety in composition and structure. Among these clusters are included many structurally characterized species that contain core units of the stoichiometries Cu_4S_6,[1-7] Cu_4S_8,[8,9] Cu_5S_6,[10] Cu_5S_7,[11] Cu_8S_{12},[12-14] $Cu_8S_{12}Cl$,[15,16] and Cu_3S_6.[17]

Our studies on aggregates with the Cu_4S_6[2] and Cu_8S_{12}[12-14] frameworks have been directed particularly in analyzing the possible factors that dictate the formation of structurally different cores with the same Cu/S ratio. In previous reports,[2,14] we have suggested that with nonchelating ligands such as the RS^- thiolates a Cu:S ratio of 2:3 favors the formation of the Cu_4S_6 "adamantane" type of core. The long S–S distances inherent in the adamantane structure (~4.0 Å with "normal" Cu–S bond lengths of ca. 2.3 Å) preclude the ability of normal bidentate chelates with small intraligand S–S distances (S–S "bite" distances ~3.0 Å) to span the edges of the S_6 octahedron in the Cu_4S_6 core. As a consequence various dinegative 1,1-dithiolate chelates with "bites" close to 3.0 Å invariably form the $[Cu_8L_6]^{4-}$ "cubane" clusters with the Cu_8S_{12} core and idealized T_h symmetry. In the latter the trigonal-planar coordination of the CuS_3 structural and the Cu–S and Cu–Cu nearest neighbor distances are similar to those in the Cu_4S_6 cores.

The stabilities of the $[Cu_4L_3]^{2-}$ and $[Cu_8L_6]^{4-}$ clusters become comparable when the sulfur chelating ligands are characterized by relatively long S–S intraligand distances. Such is the case for the sulfur "rich" derivative of the 1,1-dicarbo-*tert*-butoxyethylene-2,2-dithiolate ligand, $[R_2DED]^{2-}$.

We have shown[18] that the transformation of $[Cu_4L_3]^{2-}$ to $[Cu_8L_6]^{4-}$ (L = $[S\text{-}t\text{-}Bu_2DED]^{2-}$) is affected by the nature of the counterion and relatively weak interionic interactions.

The coordinated $[t\text{-}Bu_2DED]^{2-}$ ligand also can undergo protonation at the "methine" carbon and is transformed to the dithio acid, $[H\text{-}t\text{-}Bu_2DED]^-$, ligand. The latter reaction can be used to explore the structural changes that the $[Cu_8L_6]^{4-}$ cluster (L = *t*-Bu_2DED) undergoes as the ligands are protonated sequentially. In a previous, short communication, we reported[19] on the acid–base

---

*To whom correspondence should be addressed at The University of Michigan.

(1) Griffith, E. H.; Hunt, G. W.; Amma, E. L. *J. Chem. Soc., Chem. Commun.* **1972**, 432.
(2) Coucouvanis, D.; Murphy, C. N.; Kanodia, S. K. *Inorg. Chem.* **1980**, *19*, 2993.
(3) Dance, I. G.; Calabrese, J. C. *Inorg. Chim. Acta* **1976**, *19*, L41.
(4) Siiman, O.; Huber, C. P.; Post, M. L. *Inorg. Chim. Acta* **1977**, *25*, L11.
(5) Betz, P.; Krebs, B.; Henkel, G. *Angew. Chem., Int. Ed. Engl.* **1984**, *23*, 311.
(6) Muller, A.; Romer, M.; Krickemeyer, E.; Bogge, H. *Naturwissenschaften* **1984**, *71*, 43.
(7) Henkel, G.; Krebs, B.; Betz, P.; Fietz, H.; Saatkamp, K. *Angew. Chem., Int. Ed. Engl.* **1988**, *27*, 1326.
(8) Hesse, R. *Ark. Kemi* **1963**, *20*, 481.
(9) Lawton, S. L.; Rohrbaugh, W. J.; Kokotaillo, G. T. *Inorg. Chem.* **1972**, *11*, 612.
(10) Dance, I. G. *J. Chem. Soc., Chem. Commun.* **1976**, 103.
(11) Dance, I. G. *J. Chem. Soc., Chem. Commun.* **1976**, 68.
(12) McCandlish, L. E.; Bissel, E. C.; Coucouvanis, D.; Fackler, J. P.; Jr.; Knox, K. *J. Am. Chem. Soc.* **1968**, *90*, 7357.
(13) Hollander, F. J.; Coucouvanis, D. *J. Am. Chem. Soc.* **1974**, *96*, 5646.
(14) Hollander, F. J.; Coucouvanis, D. *J. Am. Chem. Soc.* **1977**, *99*, 6268.
(15) Birker, P. J. M. W. L.; Freeman, H. C. *J. Chem. Soc., Chem. Commun.* **1976**, 312.
(16) Schugar, H. J.; Ou, C.; Thick, J. A.; Potenza, J. A.; Lalancette, P. A.; Furey, W. *J. Am. Chem. Soc.* **1976**, *98*, 3047.
(17) Henkel, G.; Betz, P.; Krebs, B. *J. Chem. Soc., Chem. Commun.* **1984**, 314.
(18) Kanodia, S.; Coucouvanis, D. *Inorg. Chem.* **1982**, *21*, 469.
(19) Coucouvanis, D.; Swenson, D.; Baenziger, N. C.; Pedelty, R.; Caffery, M. L. *J. Am. Chem. Soc.* **1977**, *99*, 8097.

0020-1669/89/1328-2829$01.50/0 © 1989 American Chemical Society

behavior of the $[Cu_8(t\text{-}Bu_2DED)_6]^{4-}$ cluster and on the structure of one of the protonation products, $[Cu_{10}(H\text{-}t\text{-}Bu_2DED)_6(t\text{-}Bu_2DED)_2]$. In this paper, we report in detail on the structure of the latter cluster and on our studies of the other protonation derivatives of the $[Cu_8(t\text{-}Bu_2DED)_6]^{4-}$ cluster.

Experimental Section

General Procedures and Techniques. The chemicals in this research were used as purchased. $K_4Cu_8(t\text{-}Bu_2DED)_6$ and $(Ph_4P)_4[Cu_8(Et_2DED)_6]$ were prepared by previously published procedures.[14,18] Dichloromethane, CH_2Cl_2, and acetonitrile were distilled from CaH_2 before use. Elemental analyses for CHN on samples dried under vacuum for 6 h were carried out by the analytical services laboratory of the chemistry department of the University of Iowa. Copper analysis was carried out by EDTA titrations using murexide as an indicator. Sulfur and phosphorus analyses were obtained from Clark Microanalytical Laboratory, Urbana, IL.

Physical Methods. Visible and UV electronic spectra were obtained on a Cary Model 118 spectrophotometer. Infrared spectra were recorded on a Beckman 20A IR spectrometer in either pressed potassium bromide disks or Nujol or hexachlorobutadiene mulls between potassium bromide plates. Conductivity measurements were carried out in purified and distilled dichloroethane, spectrophotometric grade acetone, and CH_3CN by using an Industrial Instrument Inc. Model RC 16B2 conductivity bridge and a Beckman Instruments Inc. conductivity cell. Molecular weights were determined by using a Mechrolab Model 301A vapor-pressure osmometer calibrated with benzil. Potentiometric titrations were performed with a Fisher Accummet pH meter Model 210 equipped with a Corning combination electrode adapted with 2-propanol and KCl for nonaqueous titrations. Standard acid solutions were 0.1 M HCl or 0.1 M $HClO_4$ in CH_3CN. They were standarized against pure diphenylguanidine.[20] Solutions were stored at 0 °C and used within 2 days. Standard basic solutions were 0.05 M in tetraethylammonium hydroxide or 0.05 M in tetrabutylammonium hydroxide in 2-propanol. The basic solutions were standarized prior to use with benzoic acid.[21] Proton NMR spectra were obtained on a Varian HA-100 spectrometer with tetramethylsilane, TMS, as an internal standard. ^{13}C NMR spectra were obtained with a Bruker HX90E spectrometer equipped for pulse Fourier transform operation. Most spectra were obtained with broad-band proton decoupling, employing the solvent deuterium signal as an internal lock. Chemical shifts are given in parts per million, ppm, downfield from internal tetramethylsilane.

Syntheses. Tris(tetrabutylammonium) Pentakis(1,1-dicarbo-*tert*-butoxyethylene-2,2-dithiolato)(2,2-dicarbo-*tert*-butoxydithioacetato)octacuprate(I), $(Bu_4N)_3Cu_8(H\text{-}t\text{-}Bu_2DED)(t\text{-}Bu_2DED)_5$. An amount of $K_4Cu_8(t\text{-}Bu_2DED)_6$[18] (2.4 g, 0.001 mol) was suspended in 20 mL of CH_3CN and 1 equiv of $HClO_4$ (in a 0.1 M CH_3CN solution) was added slowly with stirring. The solution slowly changed in color from orange to dark green. At this stage 0.83 g (0.003 mol) of Bu_4NCl was added to the green solution. After being stirred for ca. 5 min, the solution was filtered, and the solvent was removed under reduced pressure. The crude product was dissolved in acetone and filtered, and pentane was added to incipient crystallization. When the solution was cooled to 0 °C, a green solid formed and was isolated. This solid was recrystallized from a CH_2Cl_2/*n*-pentane mixture to give dark green tetrahedral crystals in 75% yield; mp 190 °C dec.

Anal. Calcd for $C_{120}H_{217}Cu_8O_{24}N_3S_{12}$ (mol wt 2975): C, 48.40; H, 7.29; N, 1.41. Found: C, 48.29; H, 7.61; N, 1.59.

IR, selected vibrations, cm^{-1}: $\nu(C{=}O)$, 1697 (s), 1707 (s); $\nu(C{=}CS_2)$, 1468 (s), 1482 (s); $\nu(C{-}S) + \nu(C{=}C)$, 1072 (m); $\nu(C{-}S)$, 847 (w), 892 (m), 909 (m), 927 (m).

Tris(tetraphenylphosphonium) Pentakis(1,1-dicarbo-*tert*-butoxyethylene-2,2-dithiolato)(2,2-dicarbo-*tert*-butoxydithioacetato)octacuprate(I), $(Ph_4P)_3Cu_8(H\text{-}t\text{-}Bu_2DED)(t\text{-}Bu_2DED)_5$. The Ph_4P^+ salt of the monoprotonated $[Cu_8(t\text{-}Bu_2DED)_6]^{4-}$ cluster was obtained in a similar manner by using 0.1 M HCl in CH_3CN, $K_4Cu_8(t\text{-}Bu_2DED)_6$, and Ph_4PCl in a 1:1:3 molar ratio in CH_3CN. The crude product, isolated by evaporation of the solvent under reduced pressure, was recrystallized from a $CHCl_3$ solution by the addition of CS_2 to incipient crystallization and cooling to 0 °C. The dark crystals were obtained in 83% yield, mp 164 °C dec.

Anal. Calcd for $C_{144}H_{169}Cu_8O_{24}P_3S_{12}$ (mol wt 3266): C, 52.90; H, 5.21; Cu, 15.6. Found: C, 52.10; H, 5.25; Cu, 15.5.

IR, selected vibrations, cm^{-1}: $\nu(C{=}O)$, 1700 (s), 1709 (s); $\nu(C{=}CS_2)$, 1455 (s), 1489 (s); $\nu(C{-}S) + \nu(C{=}C)$, 1074 (m); $\nu(C{-}S)$, 845 (w), 889 (w), 925 (w), 927 (m).

Bis(benzyltriphenylphosphonium) Tetrakis(1,1-dicarbo-*tert*-butoxyethylene-2,2-dithiolato)bis(2,2-dicarbo-*tert*-butoxydithioacetato)octacuprate(I), $(BzPh_3P)_2Cu_8(H\text{-}t\text{-}Bu_2DED)_2(t\text{-}Bu_2DED)_4$. An amount of $K_4Cu_8(t\text{-}Bu_2DED)_6$[18] (2.55 g, 0.0012 mol) was suspended in 20 mL of CH_3CN, and 2 equiv of HCl (0.1 M in CH_3CN) was added slowly with stirring. To the green violet solution was added 0.82 g (0.0023 mol) of $BzPh_3PCl$, and after being stirred for ca. 5 min, the solution was filtered and the solvent was removed under reduced pressure. The crude product was dissolved in 30 mL of acetone, the solution was filtered, and *n*-pentane was added to incipient crystallization. When the solution was cooled to 0 °C for 12 h, violet crystals formed and were isolated, washed with several portions of diethyl ether, and dried in vacuo: yield 54%; mp 125 °C dec.

Anal. Calcd for $C_{122}H_{154}Cu_8O_{24}P_2S_{12}$ (mol wt 2956): C, 49.51; H, 5.25; S, 13.00; P, 2.09; Cu, 17.2. Found: C, 49.51; H, 5.19; S, 13.18; P, 2.00; Cu, 17.00.

IR, selected vibrations, cm^{-1}: $\nu(C{=}O)$, 1708 (s), 1733 (s); $\nu(C{=}CS_2)$, 1457 (s), 1470 (s); $\nu(C{-}S) + \nu(C{=}C)$, 1100 (m); $\nu(C{-}S)$, 847 (m), 906 (w).

Bis(1,1-dicarbo-*tert*-butoxyethylene-2,2-dithiolato)hexakis(2,2-dicarbo-*tert*-butoxydithioacetato)decacopper(I), $Cu_{10}(H\text{-}t\text{-}Bu_2DED)_6(t\text{-}Bu_2DED)_2$. An amount of $K_4Cu_8(t\text{-}Bu_2DED)_6$[18] (2.6 g, 0.0013 mol) was suspended in 20 mL of CH_3CN, and 4 equiv of HCl (0.1 M in CH_3CN) was added slowly with stirring. The solution changed in color from orange to dark green to violet to dark red. After being stirred for ca. 5 min, the solution was filtered and the solvent was removed under reduced pressure. The crude product was dissolved in $CHCl_3$, and pentane was added to incipient crystallization. When the solution was allowed to stand at 0 °C, red crystals formed. These crystals were isolated (mp 128 °C dec) in 80% yield.

Anal. Calcd for $C_{96}H_{150}Cu_{10}O_{32}S_{16}$ (mol wt 2961): C, 38.90; H, 5.06; S, 17.29; Cu, 21.44. Found: C, 39.13; H, 5.29; S, 17.05; Cu, 21.2.

IR, selected vibrations, cm^{-1}: $\nu(C{=}O)$, 1599 (m), 1751 (m); $\nu(C{-}S)$, 933 (w), 976 (w), 1009 (w).

Tris(tetraphenylphosphonium) Pentakis(1,1-dicarboethoxyethylene-2,2-dithiolato)(2,2-dicarboethoxydithioacetato)octacuprate(I), $(Ph_4P)_3[Cu_8(H\text{-}Et_2DED)(Et_2DED)_5]$. An amount of $(Ph_4P)_4[Cu_8(Et_2DED)_6]$[14] (0.984 g, 0.003 mol) was suspended in 20 mL of CH_3CN, and to that was added 3 equiv of $HClO_4$ (in a 0.1 M CH_3CN solution) slowly with stirring. The dark green solution that was so obtained was diluted with 200 mL of anhydrous ether. The Ph_4PClO_4 that precipitated was filtered off, and the filtrate was evaporated to near dryness under reduced pressure. The residue was dissolved in the minimum amount of acetone required, and the acetone solution was added with stirring to 250 mL of anhydrous ether. A dark green crystalline powder formed and was isolated: mp 96–98 °C; 75% yield.

Anal. Calcd for $C_{120}H_{121}Cu_8O_{24}P_3S_{12}$ (mol wt. 2930): C, 49.14; H, 4.09; Cu, 17.34. Found: C, 49.27; H, 4.11; Cu, 17.2.

IR, selected vibrations, cm^{-1}: $\nu(C{=}O)$, 1710 (s), 1662 (m); $\nu(C{=}CS_2)$, 1462 (s); $\nu(C{-}S) + \nu(C{=}C)$, 1030 (s), 995 (s); $\nu(C{-}S)$, 890 (m), 907 (sh).

Bis(tetraphenylphosphonium) Tetrakis(1,1-dicarboethoxyethylene-2,2-dithiolato)bis(2,2-dicarboethoxydithioacetato)octacuprate(I), $[Cu_8(H\text{-}Et_2DED)_2(Et_2DED)_4]$. The diprotonated cluster was obtained by a procedure very similar to the one described above for the monoprotonated cluster, using 2 mmol of acid/mmol of $(Ph_4P)_4[Cu_8(Et_2DED)_6]$. The olive green crystalline product was obtained in 77% yield; mp 82–85 °C.

Anal. Calcd for $C_{96}H_{102}Cu_8O_{24}P_2S_{12}$ (mol wt 2592): C, 44.44; H, 3.96; Cu, 19.60. Found: C, 44.29; H, 3.80; Cu, 19.3.

IR, selected vibrations, cm^{-1}: $\nu(C{=}O)$, 1715 (s), 1648 (m); $\nu(C{=}CS_2)$, 1460 (s); $\nu(C{-}S) + \nu(C{=}C)$, 1025 (s), 995 (m); $\nu(C{-}S)$, 890 (m), 908 (sh).

Tetraphenylphosphonium Tris(1,1-dicarboethoxyethylene-2,2-dithiolato)tris(2,2-dicarboethoxydithioacetato)octacuprate(I), $(Ph_4P)[Cu_8(H\text{-}Et_2DED)_3(Et_2DED)_3]$. The triprotonated cluster was obtained by a procedure very similar to the one described above for the monoprotonated cluster, using 3 mmol of acid/mmol of $(Ph_4P)_4[Cu_8(Et_2DED)_6]$. The dark red crystalline powder was obtained in 66% yield; mp 75 °C dec.

Anal. Calcd for $C_{72}H_{83}Cu_8O_{24}PS_{12}$ (mol wt 2254): C, 38.34; H, 3.71; Cu, 22.54. Found: C, 37.70; H, 3.55; Cu, 21.6.

IR, selected vibrations, cm^{-1}: $\nu(C{=}O)$, 1740 (s), 1668 (s), 1630 (s); $\nu(C{=}CS_2)$, 1472 (s); $\nu(C{-}S) + \nu(C{=}C)$, 1020 (s); $\nu(C{-}S)$, 890 (w), 910 (sh).

Deuterated Clusters. The $Cu_{10}(D\text{-}t\text{-}Bu_2DED)_6(t\text{-}Bu_2DED)_2$ cluster was obtained by the reaction of $K_4Cu_8(t\text{-}Bu_2DED)_6$[18] (1.5 g; 0.006 mol suspended in 6 mL of acetone-d_6 under a N_2 atmosphere) with a solution

---

(20) Huber, W. *Titrations in Non-Aqueous Solvents*; Academic Press: New York, 1967.

(21) Gyenes, I. *Titrations in Non-Aqueous Media*; D. Van Nostrand Co., Inc.: Princeton, NJ, 1968.

Table I. Molecular Weight and Conductivity Data for the $(Bu_4N)_4Cu_8(Et_2DED)_6$ (A), $(Ph_4P)_3Cu_8(Et_2DED)_5(H\text{-}Et_2DED)$ (B), $(Ph_4P)_2Cu_8(Et_2DED)_4(H\text{-}Et_2DED)_2$ (C), and $(Ph_4P)Cu_8(Et_2DED)_3(H\text{-}Et_2DED)_3$ (D) Clusters

CH_3CN				acetone				1,2-$C_2H_4Cl_2$			
M_o[a]	M_c[b]	M_o/M_c	Λ[c]	M_o[a]	M_c[b]	M_o/M_c	Λ[c]	M_o[a]	M_c[b]	M_o/M_c	Λ[c]
$(Bu_4N)_4Cu_8(Et_2DED)_6$[d]											
0.017	0.005	3.42	204.2	0.009	0.005	1.74	33.06				
0.030	0.010	3.00	173.9	0.014	0.010	1.46	25.84	0.012	0.010	1.11	2.94
0.043	0.015	2.90	150.7	0.021	0.015	1.40	21.74	0.017	0.015	1.15	2.36
0.050	0.020	2.87	145.9	0.027	0.020	1.35	18.77	0.021	0.020	1.06	2.16
$(Ph_4P)_3Cu_8(Et_2DED)_5(Et_2HDED)$											
0.017	0.005	3.28	198.6	0.012	0.005	2.35	98.5	0.008	0.005	1.66	17.8
0.030	0.010	3.00	168.3	0.019	0.10	1.93	77.1	0.012	0.010	1.16	14.2
0.043	0.015	2.85	150.4	0.024	0.015	1.58	64.9	0.015	0.015	1.00	13.6
0.055	0.020	2.74	134.1					0.021	0.020	1.03	12.4
$(Ph_4P)_2Cu_8(Et_2DED)_4(Et_2HDED)_2$											
0.012	0.005	2.31	146.3	0.012	0.005	2.40	86.7	0.009	0.005	1.73	15.8
0.023	0.010	2.30	125.8	0.018	0.010	1.80	73.2	0.015	0.010	1.50	13.5
0.034	0.015	2.27	111.9	0.026	0.015	1.70	63.6	0.020	0.015	1.30	13.3
0.043	0.020	2.17	100.5	0.029	0.020	1.45	55.4	0.024	0.020	1.19	12.3
$(Ph_4P)Cu_8(Et_2DED)_3(Et_2HDED)_3$											
0.011	0.005	2.06	121.5	0.011	0.005	2.00	66.0				
0.022	0.010	2.17	108.0	0.014	0.010	1.43	58.8	0.013	0.010	1.35	11.7
0.032	0.015	2.13	96.3	0.023	0.015	1.52	55.0	0.016	0.015	1.06	10.4
0.042	0.020	2.06	88.7	0.027	0.020	1.37	53.4	0.020	0.020	1.00	9.4

[a] M_o = moles of particles per liter of solution. The entries were obtained with reference to a calibration plot constructed from data for benzil at 37 °C. M_c = moles of complex per liter of solution. [b] Concentrations (M_c = mol L^{-1}) based on molecular weights of 2882, 2933, 2595, and 2256 for A–D, respectively. [c] Molar conductance, Ω^{-1} cm^{-1}. The equivalent conductances Λ_0 in CH_3CN obtained from the extrapolation of Λ vs $c^{1/2}$ plots were 270, 194, and 153 Ω^{-1} cm^{-1}, respectively, for B–D. Similar plots for acetone yield Λ_0 values of 120, 102, and 74 Ω^{-1} cm^{-1}, respectively, for B–D. [d] Assuming a molecular weight of 1441 for this complex, values for M_o/M_c less than unity are observed for acetone and 1,2-dichloroethane solutions.

Table II. Electronic Spectral Data for the $[Cu_8(L)_{6-n}(H\text{-}L)_n]^{-(4-n)}$ Clusters (n = 0, 1, 2) and for $[Cu_{10}(H\text{-}L)_6(L)_2]$ (L = $[S_2C{=}C(COO\text{-}t\text{-}C_4H_9)_2]^{2-}$)

complex	λ, nm	ε, L mol^{-1} cm^{-1}
$[Cu_8(L)_6]^{4-}$	392	70 900
	312	69 100
$[Cu_8(L)_5(H\text{-}L)]^{3-}$	600	3 110
	376	57 600
	314	60 500
$[Cu_8(L)_4(H\text{-}L)_2]^{2-}$	554	5 670
	366	52 400
	304	51 800
$[Cu_{10}(H\text{-}L)_6(L)_2]$	364	65 500
	266 (sh)	~66 000

of 0.2 mL of 70% $DClO_4$ in 6 mL of acetone-d_6 (0.024 mol). After the slow addition of the acid solution, the solvent was removed and the complex was crystallized and characterized as described for the protonated analogue.

$(Ph_4P)[Cu_8(D\text{-}Et_2DED)_3(Et_2DED)_3]$ was obtained by a similar procedure using $(Ph_4P)_4Cu_8(Et_2DED)_6$ and 70% $DClO_4$. After the acidification step, the Ph_4PClO_4 that precipitated out of solution was filtered off, and the solution of the deuterated product was poured into 500 mL of anhydrous ether. A red brown microcrystalline powder was obtained in 78% yield and was characterized as described previously for the protonated analogue.

X-ray Diffraction Measurements. Collection and Reduction of Data and Structure Refinement Procedures. Single crystals of $[Cu_{10}(H\text{-}t\text{-}Bu_2DED)_6(t\text{-}Bu_2DED)_2]$ (III) were obtained as red prisms by the slow diffusion of pentane into a chloroform solution of the complex. One of these crystals was mounted on a glass fiber, was coated with Krylon, and was used for cell dimension measurements and data collection. Details concerning the crystal characteristics, the data collection, and the structure refinement are shown in Table III. Intensity data for III were obtained on a Picker-Nuclear four-circle diffractometer equipped with scintillation counter and pulse-height analyzer and automated by a DEC PDP8-I computer and disk with FACS-I DOS software. Graphite-monochromatized Mo Kα radiation ($2\theta_{max}$ = 12.50°) was used for data collection and cell dimension measurements (Kα, λ = 0.7107 Å). Intensity data were collected by using a θ–2θ step scan technique. The scan width was centered on the predicted position of the Mo Kα_1 peak and expanded at the high 2θ end to allow for α_1–α_2 separation at the higher angles. Stationary-crystal, stationary-counter background measurements were made for 10 s at each end of the scan range. Throughout the data collection, three standard reflections were monitored every 100 reflections to monitor crystal and instrumental stability. No crystal decay was observed. Accurate cell parameters were obtained from the least-squares refinement on the 2θ, ϕ, χ, and ω values of 25 manually centered reflections with 2θ values between 25 and 40°. The raw data were reduced to net intensities, estimated standard deviations were calculated on the basis of counting statistics, Lorentz–polarization corrections were applied, and equivalent reflections were averaged. The estimated standard deviation of the structure factor was taken as the larger of that derived from counting statistics and that derived from the scatter of multiple measurements.

The least-squares program used minimizes $\sum w(\Delta|F|)^2$. The weighting function used throughout the refinement of the structure gives zero weight to those reflections with $F^2 < 3\sigma(F^2)$ and $w = 1/\sigma^2(F)$ to all others ($\sigma^2(F^2) = (pF^2)^2 + \sigma_1{}^2(F^2)$ (from counting statistics),[22] where p = 0.04.

Table III. Summary of Crystal Data, Intensity Collection Data, and Structure Refinement Data for $Cu_{10}S_{16}O_{32}C_{96}H_{150}$

chem formula	$Cu_{10}S_{16}O_{32}C_{96}H_{150}$
MW	2961
space group	$P\bar{1}$
a, Å	14.435 (3)
b, Å	16.979 (3)
c, Å	14.843 (3)
α, deg	98.15 (4)
β, deg	108.09 (3)
γ, deg	85.24 (3)
Z	1
d_{obs},[a] g/cm^3	1.51
d_{calc} g/cm^3	1.53
cryst dimens, mm	0.44 × 0.13 × 0.25
radiation	Mo Kα
μ, cm^{-1}	18.8
data collecd	$+h\pm k\pm l$
$2\theta_{max}$(deg)	40
no. of unique reflcns	6409
no. of reflcns $I > 3\sigma(I)$	4284
no. of variables	373
R, R_w[c]	0.067, 0.070

[a] Density determined by flotation in a hexachlorobutadiene–pentane mixture. [b] λ = 0.71069 Å. [c] $R = \sum(F_o - |F_c|)/\sum F_o$; $R_w = \sum(F_o - |F_c|)^2/\sum F_o{}^2)^{1/2}$.

---

(22) Grant, D. F.; Killean, R. C. G.; Lawrence, J. L. *Acta Crystallogr., Sect. B* **1969**, *B25*, 374.

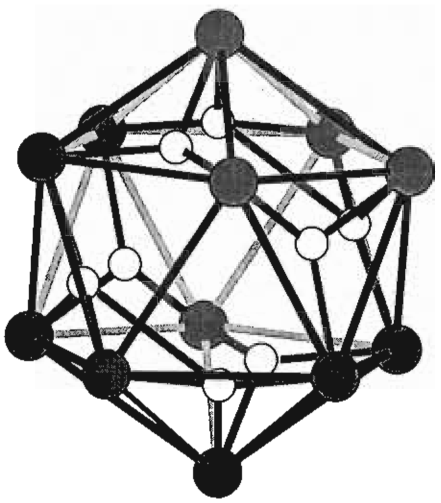

Figure 1. Cu_8S_{12} core in the $[Cu_8(L)_6]^{4-}$ cubanes.

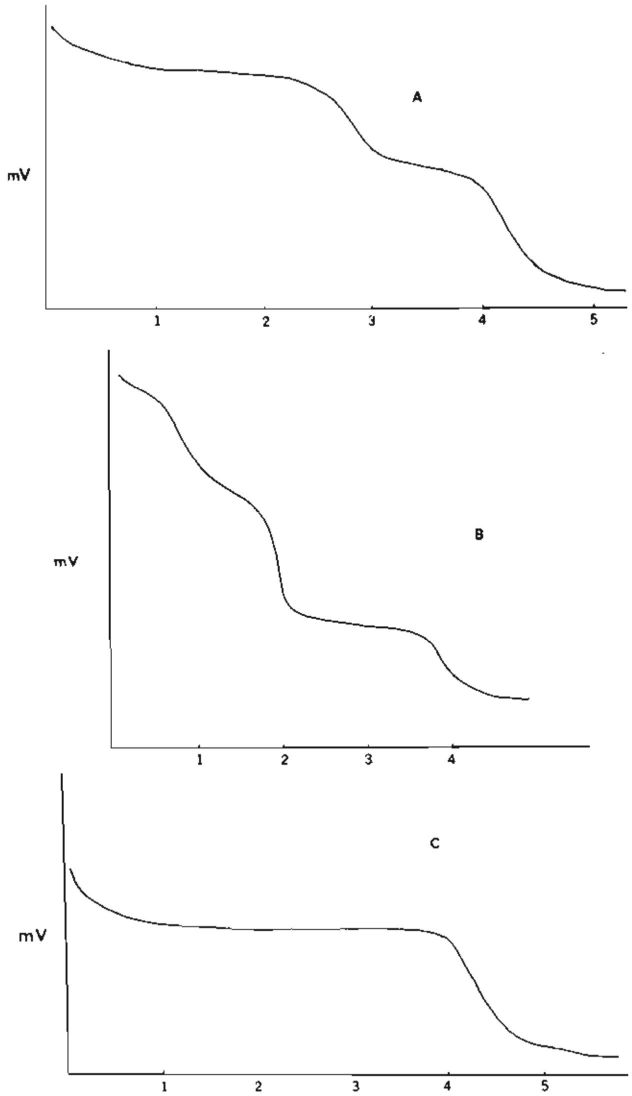

Figure 2. Potentiometric titrations of $(Ph_4P)_3Cu_8(t\text{-BuDED})_5(H\text{-}t\text{-BuDED})$ (A), $(BzPh_3P)_2Cu_8(t\text{-BuDED})_4(H\text{-}t\text{-BuDED})_2$ (B), and $(BzPh_3P)_4Cu_8(t\text{-BuDED})_6$ (C) with Bu_4NOH in CH_3CN solution. Values on the abscissa represent the number of equivalents of base added.

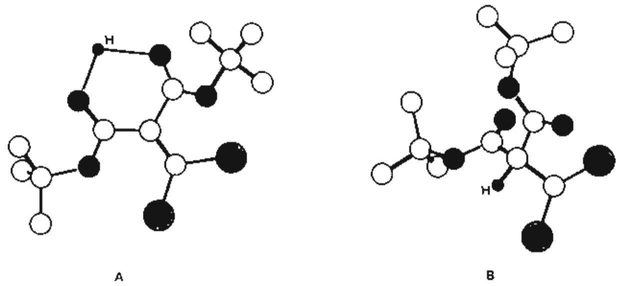

Figure 3. Possible protonation sites within the R_2DED ligands.

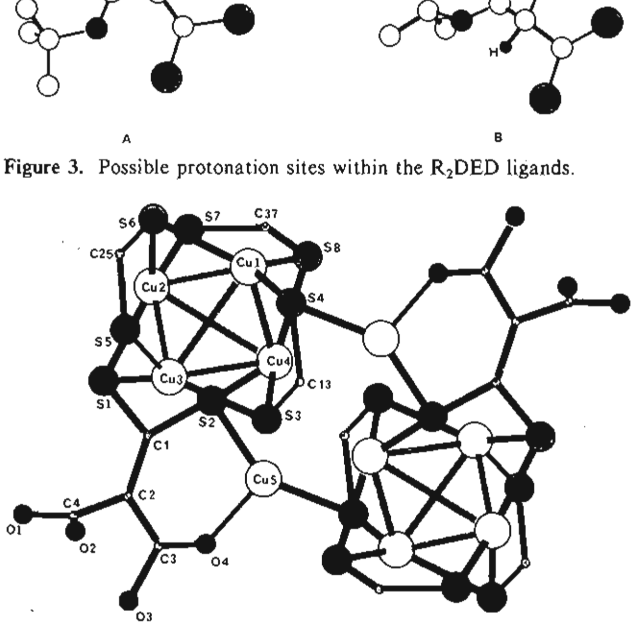

Figure 4. Structure of the inner core of the $[Cu_{10}(H\text{-}t\text{-}Bu_2DED)_6(t\text{-}Bu_2DED)_2]$ cluster. For clarity, only the CS_2 moieties of the protonated ligands are shown. For the bridging unprotonated ligand, the *tert*-Butyl groups also have been omitted for clarity. The structure was drawn from atomic coordinates on a Macintosh Plus computer using the program Molecular Editor.

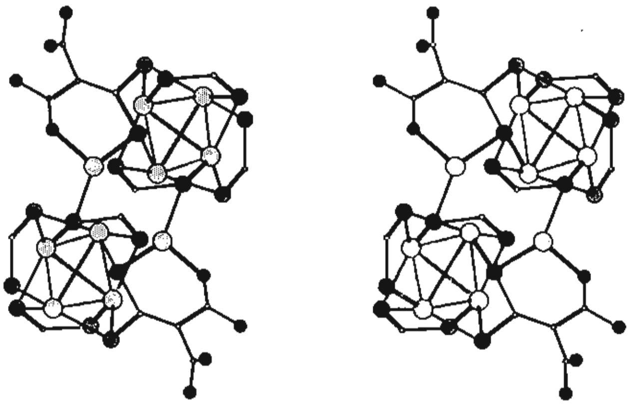

Figure 5. Stereoview of the $[Cu_{10}(H\text{-}t\text{-}Bu_2DED)_6(t\text{-}Bu_2DED)_2]$ core as shown in Figure 4.

The atomic scattering factors of the neutral non-hydrogen atoms were taken from the tables of Doyle and Turner,[23] and real and imaginary dispersion corrections[24] were applied to all of them. The spherical hydrogen scattering factor tables of Stewart, Davidson, and Simpson[25] were used. Absorption corrections were applied to the data by using the analytical program ABSORB,[26] which uses the analytical method of de Meulenaer and Tompa.[27]

Determination of the Structure. The structure of III was determined by using data collected to $2\theta_{max} = 40°$. A three-dimensional Patterson synthesis map was solved in the space group $P\bar{1}$ to yield the positions of three Cu atoms. The other non-hydrogen atoms were located on subsequent Fourier syntheses following least-squares refinements. The decanuclear cluster is located on a crystallographic center of symmetry. The final least-squares refinement of 77 non-hydrogen atoms, with the 75 hydrogen atoms included in the structure factor calculation but not refined, resulted in a R value of 0.067. In the final refinement the five

---

(23) Doyle, P. A.; Turner, P. S. *Acta Crystallogr. Sect. A* **1968**, *A24*, 390.

(24) Cromer, D. T.; Liberman, D. *J. Chem. Phys.* **1970**, *53*, 1891.

(25) Stewart, R. F.; Davidson, E. R.; Simpson, W. T. *J. Chem. Phys.* **1965**, *42*, 3175.

(26) Templeton, L.; Templeton, D. *Abstracts of Papers*; American Crystallography Society Meeting, Storrs, CT; Abstract E10, p 143. Modified for local use by F. J. Hollander.

(27) de Meulenaer, J.; Tompa, H. *Acta Crystallogr.* **1965**, *19*, 1014.

Table IV. Fractional Atomic Coordinates[a] and Equivalent Isotropic Thermal Parameters for the Non-Hydrogen Atoms in $[Cu_{10}(H\text{-}t\text{-}Bu_2DED)_6(t\text{-}Bu_2DED)_2]$

atom	*x*	*y*	*z*	*B*(11), Å^2	atom	*x*	*y*	*z*	*B*(11), Å^2
Cu(1)	−0.2171 (1)	0.11690 (9)	0.0397 (1)	2.65 (7)	C(11)	0.443 (1)	0.0703 (9)	0.122 (1)	6.3 (4)
Cu(2)	−0.1068 (1)	0.15636 (9)	0.2181 (1)	2.88 (7)	C(12)	0.509 (1)	0.062 (1)	0.300 (1)	6.5 (4)
Cu(3)	−0.0509 (1)	0.21533 (8)	0.0854 (1)	2.25 (7)	C(13)	−0.1308 (8)	0.1345 (7)	−0.1254 (8)	2.7 (2)
Cu(4)	−0.0444 (1)	0.03885 (9)	0.0696 (1)	2.42 (7)	C(14)	−0.1119 (8)	0.1709 (7)	−0.2046 (8)	2.9 (2)
Cu(5)	0.2009 (1)	−0.03398 (8)	0.1804 (1)	2.00 (7)	C(15)	−0.1939 (9)	0.1585 (8)	−0.2985 (9)	3.7 (3)
S(1)	0.0338 (2)	0.2167 (2)	0.2409 (2)	2.3 (1)	C(16)	−0.0916 (9)	0.2572 (7)	−0.1720 (8)	3.6 (3)
S(2)	0.0831 (2)	0.0445 (2)	0.2099 (2)	2.1 (1)	C(17)	0.039 (1)	0.354 (1)	−0.132 (1)	7.1 (4)
S(3)	−0.0234 (2)	0.1212 (2)	−0.0285 (2)	2.0 (1)	C(18)	0.142 (2)	0.338 (1)	−0.140 (2)	11.5 (6)
S(4)	−0.2453 (2)	0.1484 (2)	−0.1113 (2)	1.9 (1)	C(19)	0.039 (1)	0.377 (1)	−0.030 (1)	8.1 (5)
S(5)	−0.1565 (2)	0.3190 (2)	0.0568 (2)	2.8 (1)	C(20)	−0.016 (2)	0.408 (1)	−0.200 (2)	10.8 (6)
S(6)	−0.2567 (2)	0.2155 (2)	0.1429 (2)	2.6 (1)	C(21)	−0.281 (1)	0.221 (1)	−0.445 (1)	7.7 (4)
S(7)	−0.1399 (2)	0.0522 (2)	0.2789 (2)	4.2 (2)	C(22)	−0.379 (1)	0.207 (1)	−0.435 (1)	8.4 (5)
S(8)	−0.1902 (2)	−0.0099 (2)	0.0684 (2)	2.7 (1)	C(23)	−0.276 (2)	0.307 (2)	−0.454 (2)	16.8 (10)
O(1)	0.2719 (6)	0.2756 (5)	0.3432 (6)	4.0 (2)	C(24)	−0.248 (2)	0.162 (1)	−0.507 (2)	11.3 (7)
O(2)	0.2164 (7)	0.2917 (6)	0.1885 (7)	5.4 (2)	C(25)	−0.2421 (8)	0.3025 (7)	0.1033 (8)	2.7 (2)
O(3)	0.3713 (6)	0.1549 (5)	0.2351 (6)	4.0 (2)	C(26)	−0.3155 (8)	0.3690 (7)	0.1146 (8)	3.1 (2)
O(4)	0.2998 (6)	0.0409 (5)	0.2096 (6)	4.1 (2)	C(27)	−0.3249 (9)	0.4338 (8)	0.052 (1)	4.3 (3)
O(5)	−0.0011 (7)	0.2710 (5)	−0.1654 (6)	5.0 (2)	C(28)	−0.287 (1)	0.4039 (9)	0.220 (1)	5.1 (3)
O(6)	−0.1492 (6)	0.3068 (5)	−0.1531 (6)	4.9 (2)	C(29)	−0.3651 (9)	0.4615 (8)	−0.1103 (9)	4.2 (3)
O(7)	−0.2045 (7)	0.2195 (6)	−0.3442 (7)	5.7 (2)	C(30)	−0.267 (1)	0.490 (1)	−0.099 (1)	6.6 (4)
O(8)	−0.2386 (6)	0.0992 (5)	−0.3236 (6)	4.4 (2)	C(31)	−0.393 (1)	0.402 (1)	−0.201 (1)	9.4 (5)
O(9)	−0.3575 (6)	0.4086 (5)	−0.0363 (6)	3.8 (2)	C(32)	−0.444 (1)	0.523 (1)	−0.110 (1)	7.2 (4)
O(10)	−0.3042 (7)	0.5015 (6)	0.0884 (7)	5.7 (2)	C(33)	−0.145 (1)	0.4511 (9)	0.352 (1)	5.8 (4)
O(11)	−0.1938 (6)	0.4139 (5)	0.2538 (6)	4.7 (2)	C(34)	−0.163 (2)	0.407 (1)	0.422 (2)	10.3 (6)
O(12)	−0.3471 (8)	0.4192 (7)	0.2624 (8)	7.8 (3)	C(35)	−0.041 (1)	0.443 (1)	0.353 (1)	8.5 (5)
O(13)	−0.1924 (6)	−0.1187 (5)	0.3566 (6)	5.0 (2)	C(36)	−0.175 (2)	0.538 (1)	0.361 (2)	10.8 (6)
O(14)	−0.0478 (7)	−0.1327 (6)	0.3270 (7)	5.5 (2)	C(37)	−0.1735 (8)	−0.0175 (7)	0.1868 (8)	2.7 (2)
O(15)	−0.3589 (8)	−0.0581 (6)	0.1791 (7)	6.6 (2)	C(38)	−0.1906 (7)	−0.0999 (6)	0.2044 (7)	2.3 (2)
O(16)	−0.3161 (6)	−0.1869 (5)	0.1670 (6)	4.5 (2)	C(39)	−0.1335 (9)	−0.1191 (7)	0.3045 (8)	3.6 (3)
C(1)	0.1239 (8)	0.1421 (6)	0.2294 (7)	2.4 (2)	C(40)	−0.300 (1)	−0.1123 (8)	0.1831 (9)	4.3 (3)
C(2)	0.2138 (8)	0.1651 (6)	0.2361 (7)	2.5 (2)	C(41)	−0.154 (1)	−0.139 (1)	0.458 (1)	6.8 (4)
C(3)	0.2932 (8)	0.1138 (7)	0.2255 (8)	3.1 (2)	C(42)	−0.114 (2)	−0.220 (2)	0.459 (2)	12.1 (7)
C(4)	0.2336 (8)	0.2519 (7)	0.2510 (9)	3.3 (3)	C(43)	−0.078 (1)	−0.079 (1)	0.516 (1)	8.1 (5)
C(5)	0.303 (1)	0.3590 (9)	0.376 (1)	5.5 (3)	C(44)	−0.241 (2)	−0.125 (1)	0.491 (2)	11.0 (6)
C(6)	0.345 (2)	0.356 (1)	0.483 (1)	9.5 (5)	C(45)	−0.417 (1)	−0.2178 (9)	0.151 (1)	5.2 (3)
C(7)	0.383 (1)	0.374 (1)	0.337 (1)	8.6 (5)	C(46)	−0.399 (2)	−0.306 (1)	0.137 (2)	12.1 (7)
C(8)	0.220 (1)	0.415 (1)	0.355 (1)	9.0 (5)	C(47)	−0.447 (1)	−0.192 (1)	0.234 (1)	8.0 (5)
C(9)	0.466 (1)	0.1152 (8)	0.2224 (9)	4.4 (3)	C(48)	−0.484 (2)	−0.193 (1)	0.063 (2)	12.3 (7)
C(10)	0.526 (1)	0.187 (1)	0.234 (1)	7.5 (4)					

[a] Calculated standard deviations are indicated in parentheses.

copper atoms and the eight sulfur atoms in the asymmetric unit were refined with anisotropic temperature factors. The carbon and oxygen atoms were refined with isotropic temperature factors. During the last cycle of refinement, all parameter shifts were less than 20% of their esd's.

Crystallographic Results. A summary of crystal data, intensity collection and structure refinement data for III is given in Table III. The final atomic positional and thermal parameters for III with standard deviations as calculated from the inverse least-squares matrix are given in Table IV. Selected intramolecular distances and angles are given in Tables V and VI. The atom-labeling scheme for the core in III, a stereopair drawing for III, and the numbering scheme for the two chemically distinct ligands are shown in Figures 4–6, respectively.

Results and Discussion

The $[Cu_8(R_2DED)_6]^{4-}$ clusters (R = C_2H_5 (I), $t\text{-}C_4H_9$ (II)) are obtained readily[14,18] by the reaction of the $K_2(R_2DED)$ salts with $Cu(CH_3CN)_4ClO_4$[28] in CH_3CN solution. The structure of the $[Cu_8(Et_2DED)_6]^{4-}$ cluster has been determined[14] and has revealed the Cu_8S_{12} cubic core (Figure 1). The latter appears to be one of the preferred structural units for clusters of Cu(I) with the Cu_4L_3 stoichiometry, where L = 1,1- or 1,2-dithiolene ligands. Such clusters include the structurally characterized $[Cu_8(Dts)_6]^{4-}$[14,29] and $[Cu_8(MNT)_6]^{4-}$[12] anions. The octanuclear structure proposed for the $[Cu_8(t\text{-}Bu_2DED)_6]^{4-}$ anion (as opposed to the tetranuclear $[Cu_4(t\text{-}Bu_2DED)_3]^{2-}$ cluster) is supported by molecular weight determinations. Thus the apparent molecular weight of the $BzPh_3P^+$[29] salt of II in 1,2-dichloroethane solution varies as a function of concentration. At concentrations greater than 0.08 M, however, it is constant at 3600 ± 70. The data is consistent with nearly complete ionic association at higher concentrations, and the apparent molecular weight agrees well with the calculated molecular weight of 3666 calculated for the $(BzPh_3P)_4$(II) cluster. Detailed molecular weight and conductivity studies of $(Bu_4N)_4$(I), in solvents of varing polarity as a function of concentration, also indicate (Table I) that I in solution retains the same nuclearity it shows in the crystalline state. Potentiometric titrations of I and II with standard solutions of $HClO_4$ in CH_3CN show inflections at 1 and 6 equiv of acid added and also support the assumed octanuclear molecularity.

Addition of aliquots of HCl or $HClO_4$ solutions (0.1 M in CH_3CN) to solutions of either I or II in CH_3CN result in pronounced color changes. Crystalline, well-defined products were obtained following the addition of 1, 2, and 3 equiv of acid to I and 1, 2, and 4 equiv to II. The analytical data for these compounds are consistent with the removal of one cation from salts of either I or II for each equivalent of acid added to the complex anions. Addition of the third proton to I results in the formation of the corresponding triprotonated $[Cu_8(H\text{-}Et_2DED)_3(Et_2DED)_3]^-$ cluster, which can be isolated in crystalline form as a Ph_4P^+ salt. In contrast, the $[Cu_8(H\text{-}t\text{-}Bu_2DED)_3(t\text{-}Bu_2DED)_3]^-$ anion is rather unstable, and pure salts of this anion could not be isolated. A probable reason for this apparent instability may be the superior stability of the neutral $[Cu_{10}(H\text{-}t\text{-}Bu_2DED)_6(t\text{-}Bu_2DED)_2]$ cluster (III) that forms in 80% yield upon the addition of 4 equiv of acid to solutions of II.

A detailed study of the colligative properties of the protonation products of I (as Ph_4P^+ salts) was carried out in CH_3CN, acetone,

---

(28) Hemmerick, P.; Sigwart, C. *Experientia* **1963**, *19*, 488.

(29) Abbreviations used: $BzPh_3P^+$ = benzyltriphenylphosphonium cation, $(C_7H_7)(C_6H_5)_3P^+$; Ph_4P^+ = tetraphenylphosphonium cation, $(C_6H_5)_4P^+$; Et_4N^+ = tetraethylammonium cation, $(C_2H_5)_4N^+$; Dts = dithiosquarate dianion, $(O_2C_4S_2)^{2-}$; MNT = 1,2-dicyanoethylenedithiolate dianion, $[S_2C_2(CN)_2]^{2-}$; Et_2Dtc = diethyldithiocarbamate anion, $(Et_2NCS_2)^-$; Dtp = diisopropyl dithiophosphate anion, $[(i\text{-}PrO)_2PS_2]^-$.

Table V. Interatomic Distances (Å) and Angles (deg) within the $Cu_{10}S_{16}O_2$ Core of the $[Cu_{10}(H\text{-}t\text{-}Bu_2DED)_6(t\text{-}Bu_2DED)_2]$ Cluster

Distances			
Cu(1)–Cu(2)	2.656 (2)	Cu(2)–S(1)	2.259 (3)
Cu(1)–Cu(3)	2.888 (2)	Cu(2)–S(6)	2.322 (3)
Cu(1)–Cu(4)	2.664 (2)	Cu(2)–S(7)	2.243 (3)
Cu(1)–Cu(5)	3.438 (2)	Cu(3)–S(1)	2.250 (3)
Cu(2)–Cu(3)	2.686 (2)	Cu(3)–S(3)	2.261 (3)
Cu(2)–Cu(4)	3.056 (2)	Cu(3)–S(5)	2.230 (3)
Cu(3)–Cu(4)	2.968 (2)	Cu(4)–S(2)	2.308 (3)
Cu(4)–Cu(4)′	2.872 (3)	Cu(4)–S(3)	2.257 (3)
		Cu(4)–S(8)	2.318 (3)
Cu(1)–S(4)	2.282 (3)	Cu(5)–O(4)	1.898 (8)
Cu(1)–S(6)	2.267 (3)	Cu(5)–S(2)	2.187 (3)
Cu(1)–S(8)	2.233 (3)	Cu(5)–S(4)	2.209 (3)
S(1)–S(2)	2.958 (4)	S(5)–S(6)	3.004 (4)
S(3)–S(4)	3.075 (4)	S(7)–S(8)	3.032 (4)
Angles			
Cu(2)–Cu(1)–Cu(3)	57.79 (5)	S(2)′–Cu(5)–S(4)	148.1 (2)
Cu(2)–Cu(1)–Cu(4)	70.12 (6)	S(2)′–Cu(5)–O(4)′	99.6 (3)
Cu(2)–Cu(1)–Cu(5)	141.37 (6)	S(4)–Cu(5)–O(4)′	110.8 (3)
Cu(1)–Cu(2)–Cu(3)	65.44 (5)		
Cu(1)–Cu(2)–Cu(4)	55.07 (5)	Cu(2)–S(1)–Cu(3)	73.12 (9)
Cu(1)–Cu(3)–Cu(2)	56.77 (5)	Cu(3)–S(3)–Cu(4)	82.14 (10)
Cu(1)–Cu(3)–Cu(4)	54.11 (5)	Cu(1)–S(6)–Cu(2)	70.71 (9)
Cu(1)–Cu(4)–Cu(2)	54.81 (5)	Cu(1)–S(8)–Cu(4)	71.64 (9)
Cu(1)–Cu(4)–Cu(3)	61.40 (5)	Cu(1)–S(4)–Cu(5)	99.90 (10)
Cu(1)–Cu(4)–Cu(4)′	128.18 (6)	Cu(4)–S(2)–Cu(5)′	106.68 (10)
S(4)–Cu(1)–S(6)	114.9 (1)	Cu(2)–S(1)–C(1)	108.0 (4)
S(4)–Cu(1)–S(8)	120.3 (2)	Cu(3)–S(1)–C(1)	98.4 (3)
S(6)–Cu(1)–S(8)	123.0 (2)	Cu(4)–S(2)–C(1)	105.1 (3)
S(1)–Cu(2)–S(6)	121.1 (2)	Cu(3)–S(3)–C(13)	100.8 (4)
S(1)–Cu(2)–S(7)	131.8 (2)	Cu(4)–S(3)–C(13)	112.4 (4)
S(6)–Cu(2)–S(7)	106.0 (1)	Cu(1)–S(4)–C(13)	102.0 (4)
S(1)–Cu(3)–S(3)	122.5 (1)	Cu(1)–S(6)–C(25)	105.3 (4)
S(1)–Cu(3)–S(5)	112.8 (1)	Cu(2)–S(6)–C(25)	111.1 (4)
S(3)–Cu(3)–S(5)	124.6 (1)	Cu(3)–S(5)–C(25)	104.6 (4)
S(2)–Cu(4)–S(3)	111.2 (1)	Cu(1)–S(8)–C(37)	110.9 (4)
S(2)–Cu(4)–S(8)	118.0 (1)	Cu(4)–S(8)–C(37)	103.5 (4)
S(3)–Cu(4)–S(8)	127.1 (1)	Cu(2)–S(7)–C(37)	104.8 (4)

Table VI. Interatomic Distances (Å) and Angles (deg) within the Ligands in the $[Cu_{10}(H\text{-}t\text{-}Bu_2DED)_6(t\text{-}Bu_2DED)_2]$ Cluster

Distances			
Ligand 1			
S(1)–C(1)	1.769 (11)	C(3)–O(4)	1.228 (14)
S(2)–C(1)	1.761 (11)	C(4)–O(1)	1.323 (13)
C(1)–C(2)	1.36 (1)	C(4)–O(2)	1.177 (12)
C(2)–C(3)	1.42 (1)	O(1)–C(5)	1.491 (16)
C(2)–C(4)	1.50 (2)	O(3)–C(9)	1.522 (15)
C(3)–O(3)	1.338 (13)		
Ligand 2			
S(3)–C(13)	1.781 (11)	C(15)–O(8)	1.193 (13)
S(4)–C(13)	1.723 (11)	C(16)–O(5)	1.317 (13)
C(13)–C(14)	1.51 (2)	C(16)–O(6)	1.201 (13)
C(14)–C(15)	1.52 (2)	O(5)–C(17)	1.530 (18)
C(14)–C(16)	1.50 (2)	O(7)–C(21)	1.556 (19)
C(15)–O(7)	1.292 (14)		
Ligand 3			
S(5)–C(25)	1.649 (11)	C(27)–O(10)	1.22 (1)
S(6)–C(25)	1.719 (11)	C(28)–O(11)	1.30 (1)
C(25)–C(26)	1.51 (2)	C(28)–O(12)	1.21 (1)
C(26)–C(27)	1.51 (2)	O(9)–C(20)	1.49 (1)
C(26)–C(28)	1.52 (2)	O(11)–C(33)	1.48 (2)
C(27)–O(9)	1.27 (1)		
Ligand 4			
S(7)–C(37)	1.652 (11)	C(39)–O(14)	1.19 (1)
S(8)–C(37)	1.721 (11)	C(40)–O(16)	1.28 (1)
C(37)–C(38)	1.51 (2)	C(40)–O(15)	1.19 (1)
C(38)–C(39)	1.52 (2)	O(13)–C(41)	1.51 (2)
C(38)–C(40)	1.54 (2)	O(16)–C(45)	1.53 (2)
C(39)–O(13)	1.31 (1)		
Angles			
Ligand 1			
S(1)–C(1)–S(2)	113.9 (4)	C(3)–C(2)–C(1)	125 (1)
S(1)–C(1)–C(2)	118.3 (6)	C(4)–C(2)–C(1)	120 (1)
S(2)–C(1)–C(2)	127.8 (6)	C(3)–C(2)–C(4)	115 (1)
Ligand 2			
S(3)–C(13)–S(4)	122.7 (4)	C(15)–C(14)–C(13)	112.8 (9)
S(3)–C(13)–C(14)	113.1 (6)	C(16)–C(14)–C(13)	108.8 (9)
S(4)–C(13)–C(14)	118.3 (6)	C(15)–C(14)–C(16)	112.0 (9)
Ligand 3			
S(5)–C(25)–S(6)	126.4 (2)	C(27)–C(26)–C(25)	114.2 (9)
S(5)–C(25)–C(26)	119.1 (6)	C(28)–C(26)–C(25)	108.1 (9)
S(6)–C(25)–C(26)	114.7 (6)	C(27)–C(26)–C(28)	110.0 (9)
Ligand 4			
S(7)–C(37)–S(8)	128.0 (4)	C(39)–C(38)–C(37)	113.2 (9)
S(7)–C(37)–C(38)	118.8 (6)	C(40)–C(38)–C(37)	111.2 (9)
S(8)–C(37)–C(38)	113.2 (6)	C(39)–C(38)–C(40)	111.0 (9)

and 1,2-dichloroethane solutions (Table I). In low-polarity solvents such as 1,2-dichloroethane, the clusters are highly associated and the ratios of observed (by vapor pressure osmometry) to calculated molarities approach unity at concentrations of >0.02 M. The apparent molecular weights and conductivities of the protonated clusters, in more polar solvents and at higher dilutions, indicate a significant extent of dissociation (Table I). Similar results were obtained for the $[Cu_8(H\text{-}t\text{-}Bu_2DED)_x(t\text{-}Bu_2DED)_{6-x}]^{n-}$ clusters ($x = 1$, $n = 3$; $x = 2$, $n = 2$). For these derivatives of II, however, appropriate concentrations for complete ionic association in 1,2-dichloroethane could not be reached. The apparent molecular weights for $(Ph_4P)_3[Cu_8(H\text{-}t\text{-}Bu_2DED)(t\text{-}Bu_2DED)_5]$, (0.023 M solution) and $(BzPh_3P)_2[Cu_8(H\text{-}t\text{-}Bu_2DED)_2(t\text{-}Bu_2DED)_4]$, (0.027 M solution) at 2910 ± 70 and 2170 ± 70, respectively are considerably lower than the calculated values of 3294 and 2983 and indicate appreciable ionic dissociation. The possible dissociation of H^+ in addition to the dissociation of R_4P^+ counterions is suggested by the electronic spectra of certain of the protonated clusters. Representative electronic spectra are shown in Table II. The monoprotonated $Cu_8(H\text{-}R_2DED)(R_2DED)_5]^{3-}$ clusters are dark green with a characteristic electronic absorption near 600 nm. Solutions of the crystalline salts of the $Cu_8(H\text{-}R_2DED)_2(R_2DED)_4]^{2-}$ diprotonated clusters show a low-energy electronic absorption that shifts to lower energies with increasing dielectric of the solvent. Thus, in CH_2Cl_2, the absorption of H_2-II is found at 554 nm and the solution has a purple color. In CH_3CN solution, this absorption is found at 590 nm and the solution is green. This behavior may be attributed to the dissociation of a proton according to the equilibrium

$$\underset{\text{purple}}{[Cu_8(H\text{-}R_2DED)_2(R_2DED)_4]^{2-}} \rightleftharpoons \underset{\text{green}}{[Cu_8(H\text{-}R_2DED)(R_2DED)_5]^{3-} + H^+}$$

High dielectric media would favor an equilibrium shift to the right and deprotonation of H_2-II to H-II.

The observed molecular weight of III of 3000 ± 70 (0.0140 M solution) agrees well with the calculated value of 2961 and indicates that the neutral decanuclear cluster retains its integrity in 1,2-dichloroethane solution.

Addition of stoichiometric amounts of base (Bu_4NOH, 0.1 M in CH_3CN) to solutions of the protonated derivatives of either I or II results in the quantitative conversion of these clusters to the "parent" I and II anions. These "neutralization" reactions were monitored by potentiometric titrations (Figure 2), and the yields of the parent clusters were determined by quantitative electronic spectroscopy. The conversion of III to II also was quantitative according to

$$4[Cu_{10}(H\text{-}t\text{-}Bu_2DED)_6(t\text{-}Bu_2DED)_2] + 24OH^- \rightarrow 5[Cu_8(t\text{-}Bu_2DED)_6] + 2(t\text{-}Bu_2DED)^{2-} + 24H_2O$$

The appearance of unexpected breaks in the base titrations curves (Figure 2) was attributed to the known[30] reaction of the R_4P^+ cations with base

---

[30] Fenton, G. W.; Ingold, C. K. *J. Chem. Soc.* **1929**, 2342.

$$R_4P^+ + OH^- \rightarrow R_4POH \rightarrow R_4PO^- \rightarrow R_3PO + R^-$$

$$R + H_2O \rightarrow RH + OH^-$$

This reaction is quite slow, and several minutes were required between successive additions of base to achieve a constant potential. The reactivity of Bu_4NOH toward the $BzPh_3P^+$ cation was confirmed by the potentiometric titration of the $(BzPh_3P)_4[Cu_8(t\text{-}Bu_2DED)_6]$ salt with Bu_4NOH in CH_2Cl_2 solution (Figure 2c). In this titration an "endpoint" was observed at 4 equiv of base added. The identity of the $(Bu_4N)_4[Cu_8(t\text{-}Bu_2DED)_6]$ product that formed quantitatively was established by electronic spectroscopy and chemical analysis.

The molecular weight and conductivity data, and the acid-base reactivity of the protonated clusters H-I, H_2-I, H-II, and H_2-II strongly suggest an octanuclear structure for these clusters. Unequivocal proof for a cubic Cu_8 core in the H-I cluster also has been obtained by ^{13}C NMR spectroscopy (vide infra).

Two realistic sites of protonation can be envisioned for the coordinated $(R_2DED)^{2-}$ ligands in the clusters (Figure 3). The infrared and NMR spectra and the crystal structure determination of III (vide infra) unequivocally establish the site of protonation at the "methine" carbon (Figure 3b).

Crystal and Molecular Structure of $[Cu_{10}(H\text{-}t\text{-}Bu_2DED)_6(t\text{-}Bu_2DED)_2]$ (III). With one molecule in the triclinic unit cell, in space group $P\bar{1}$, the decanuclear cluster is required to reside on a crystallographic center of symmetry. The structure of the molecular framework (Figures 4 and 5) can be described in terms of two Cu_4 tetrahedral subunits related by the center of symmetry. Of the four ligands surrounding each of the Cu_4 subunits, three are protonated at the ethylenic carbon adjacent to the CS_2 unit ("methine" carbon) and can be considered dithio acid monoanions, $(H\text{-}t\text{-}Bu_2DED)^-$. The fourth ligand is a 1,1-ethylenedithiolate dianion, $(t\text{-}Bu_2DED)^{2-}$. The coordination geometry of the $[Cu_4(H\text{-}t\text{-}Bu_2DED)_3(t\text{-}Bu_2DED)]^-$ subunits in III is a distorted version of the one observed in the structures of the $[Cu(Et_2Dtc)]_4$[8] and $[Cu(Dtp)]_4$[9,29] clusters. The four ligands are centered above and approximately bisect each of the four faces of the distorted Cu_4 tetrahedron. On each Cu_3 face two of the copper atoms are bridged by one of the sulfur atoms, while the third copper atom is coordinated by the other sulfur atom of the chelating ligand. The $(t\text{-}Bu_2DED)^{2-}$ ligand on each subunit connects to a "bridging" copper atom by coordination via an oxygen and sulfur atoms. A third coordination site on the "bridging" copper atom is occupied by a $(H\text{-}t\text{-}Bu_2DED)^-$ ligand on the adjacent Cu_4L_4 subunit (Figure 4).

The coordination geometry around each of the copper atoms in the Cu_4S_8 subunit cores is distorted trigonal and nearly planar (Table V). The S–Cu–S angles range from 106.0 (1) to 131.8 (1)°. The deviations of the copper atoms from the appropriate S(3) planes range from 0.02 to 0.19 Å. A more pronounced distortion from trigonal coordination is found for the "bridging" copper atoms. In the CuS_2O unit the two S–Cu–O angles and the S–Cu–S angle are 99.6 (3), 110.8 (3), and 148.9 (2)° respectively, and the copper is found 0.29 Å out of the S_2O plane (Table V). The Cu–Cu distances of ligand-bridged copper atoms in the Cu_{10} core range from 2.686 (2) to 3.056 (2) Å. In the Cu_4 subunits, the shorter distances are between S-bridged Cu atoms and two of the longer distances are between the nonbridged copper atoms. These value compare with corresponding values in the $[Cu(Et_2Dtc)]_4$[8] and $[Cu(Dtp)]_4$[9] clusters that also show shorter Cu–Cu distances for the S-bridged pairs. These values are 2.658 (5) and 2.757 (5) Å and 2.74 (2) and 2.950 (5) Å, respectively, for $Cu(Et_2Dtc)]_4$[8] and $[Cu(Dtp)]_4$.[9] A wide range also is observed with the Cu–S distances in III. Within the Cu_4S_8 subunits these distances range from 2.230 (3) to 2.322 (3) Å. As expected, the shorter of these distances are found with the ligand S atoms that are bound to only one copper atom (S(5) and S(7)).

Direct evidence that protonation of ligands 2, 3, and 4 (Table VI, Figure 6) has taken place at the methine carbons is provided by the C–C–C angles around the C(14), C(26), and C(38), sp^3-hybridized, carbon atoms. For these the three C–C–C angles add up to 333.7, 332.3 and 335.4° for C(14), C(26), and C(38), respectively. For the unprotonated ligand 1, the three C–C–C angles at the corresponding sp^2 hybridized carbon atom add up to 360°. For ligand 1 the ethylenic C=C bond at 1.36 Å is distinct from the corresponding C–C bonds in ligands 2, 3, and 4. In all three of the latter ligands, this bond length is 1.51 Å.

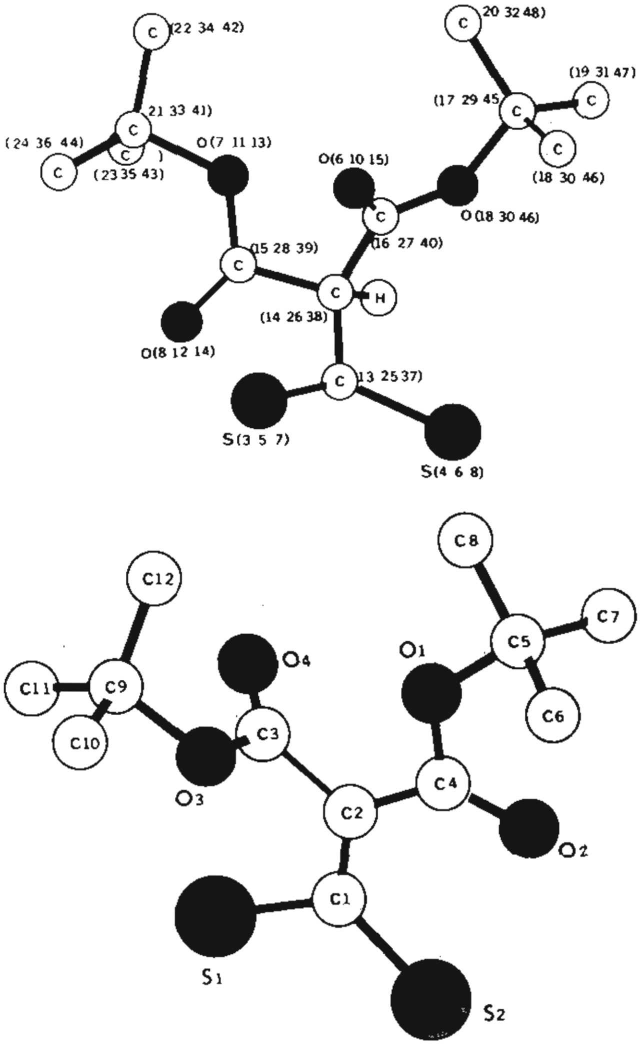

Figure 6. Numbering schemes for the three independent $[S_2CCH(COO\text{-}t\text{-}C_4H_9)_2]^-$ ligands in A (top) and the $[S_2C{=}C(COO\text{-}t\text{-}C_4H_9)_2]^{2-}$ ligand in B (bottom).

One of the carbo-*tert*-butoxy groups in the unprotonated dithiolene ligand 1 is twisted out of the $S_2C{=}C$ plane by 85.3°. This, nearly orthogonal, twist in the R_2DED ligands that has been predicted earlier[31] on the basis of infrared spectroscopy also has been observed in the structures of the $[Ni(Et_2DED)_2]^{2-}$ and $[Cu(Et_2DED)_2]^-$ anions[32] and in the structure of the $[Fe(Et_2DED)_3]^{2-}$ complex.[33]

NMR Studies. The ^1H NMR spectra of the protonated derivatives of I (H-I, H_2-I, and H_3-I) in CD_3CN show a somewhat broad resonance for the methine protons with chemical shifts within a range from 4.98 to 5.16 ppm. These chemical shifts are close to those reported[34] for the methine protons in the triethyl ester of methanetricarboxylic acid and the diethyl ester of phenylmalonic acid at 4.18 and 4.42 ppm, respectively. The relative integrated intensities of the methine signals to those of the other resonances in the Ph_4P^+ salts of H-I, H_2-I, and H_3-I are consistent

---

(31) Jensen, K. A.; Hendriksen, L. *Acta Chem. Scand.* **1968**, *22*, 1107.

(32) Coucouvanis, D.; Hollander, F. J.; Caffery, M. L. *Inorg. Chem.* **1976**, *15*, 1853.

(33) Coucouvanis, D.; Pedelty, R.; Hollander, F. J. *Inorg. Chem.* **1977**, *16*, 2691.

(34) The Sadtler Standard Spectra, Sadtler Research Lab. Inc., 3316 Spring Garden St., Philadelphia 19104.

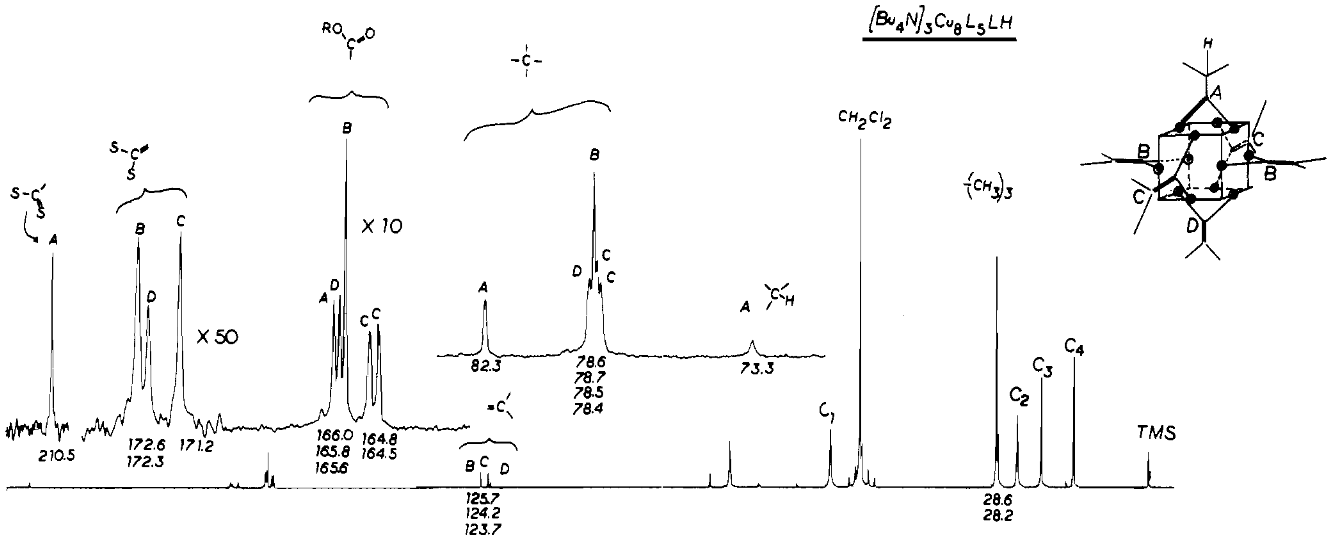

Figure 7. ^{13}C NMR spectrum of $(Bu_4N)_3[Cu_8(t\text{-}BuDED)_5(H\text{-}t\text{-}BuDED)]$ in CH_2Cl_2 solution.

with the formulation of the latter as octanuclear derivatives of I. The resonance assigned to the methine carbon in H_3-I at 5.16 ppm is absent in the ^1H NMR spectrum of D_3-I.

The ^1H NMR spectra of the H_n-II derivatives ($n = 1, 2$) show similar behavior and exhibit broad resonances in the region from 4.30 to 4.50 ppm. The spectrum of III of CD_3CN shows a simple time-averaged spectrum for the methine proton resonance absorption at 4.38 ppm. This absorption is absent in the spectrum of the deuterated complex.

All of the ^{13}C resonances in the proton-decoupled ^{13}C NMR spectrum of H-II in CH_2Cl_2 solution (Figure 7) can be assigned to a structure with the Cu_8S_{12} cubic core. In such a structure, the five t-Bu_2DED ligands are separated into three sets (2:2:1) by virtue of their location relative to the unique H-t-Bu_2DED ligand. The ^{13}C resonances of the latter, in a set labeled A, are clearly identifiable relative to the resonances attributed to the t-Bu_2DED ligands in sets B, C, and D, respectively (Figure 7). The assignments, as indicated in Figure 7, were assisted by and consistent with the ^{13}C NMR spectrum of II that has been reported previously.[18]

Summary

The synthesis of the $(R_2DED)^{2-}$ ligands and the first indications of their coordination to transition-metal ions have been reported[35] as early as 1963. Surprisingly, the coordination chemistry of these ligands has not been investigated as extensively as their versatility warrants. The ability of the $(R_2DED)^{2-}$ ligands to stabilize transition-metal ions in unusually high oxidation states already has been demonstrated in the synthesis and characterization of the Cu(III).[32] Fe(IV),[33] and Mn(IV)[36] complexes that are exceedingly more stable than the corresponding and more conventional Cu(II), Fe(III), and Mn(III) complexes. The presence of the dicarboalkoxy functional groups in these ligands allow for ternary interactions with Lewis acids. Such interactions already have been demonstrated to affect considerable structural changes as demonstrated by the transformation of $[Cu_8L_6]^{4-}$ to $2[Cu_4L_3]^{2-}$ ($L = [S\text{-}t\text{-}Bu_2DED]^{2-}$) in the presence of alkali-metal ions.[18]

The ready protonation of the coordinated $(R_2DED)^{2-}$ 1,1-dithiolene ligands and their transformation to the corresponding dithio acids add a new dimension to the coordination chemistry of the R_2DED complexes.

In the $[Cu_8(R_2DED)_6]^{4-}$ clusters, the transformation of the dinegative dithiolene ligands to the uninegative dithio acid ligands is tolerated without a basic structural change of the Cu_8S_{12} core, as long as the $[Cu_8(R_2DED)_6]$ clusters maintain a net negative charge. Once a neutral cluster is obtained, following the addition of the fourth proton, a basic structural reorganization takes place, and the $[Cu_4(H\text{-}R_2DED)_3(R_2DED)]^-$ forms with a Cu_4S_8 core structurally similar to that obtained with dithioacid ligands such as $(R_2Dtc)^-$ or $(Dtp)^-$. In the Cu_8S_{12} cubic cores obtained with the dinegative dithiolene ligands and in the Cu_4S_8 cores common with the uninegative dithioacid ligands, an optimum balance exists between the weak Cu–Cu attractive interactions[2] and the interligand, repulsive, S–S interactions. Protonation of the ligands in the $[Cu_8(R_2DED)_6]$ clusters changes this balance and result in the observed structural reorganization.

Acknowledgment. Support of this work by a grant (CH-79-0389) from the National Science Foundation is gratefully acknowledged.

Supplementary Material Available: An ORTEP diagram of III (Figure S1) and listings of positional and thermal parameters for $[Cu_{10}(H\text{-}t\text{-}Bu_2DED)_6(t\text{-}Bu_2DED)_2]$ (Table S1) (5 pages); a listing of structure factors for III (Table S2) (14 pages). Ordering information is given on any current masthead page.

---

(35) Soderback, E. *Acta Chem. Scand.* **1963**, *17*, 362.

(36) Pedelty, R. Ph.D. Thesis, University of Iowa, 1977.